







Article

New Pregnane Glycosides from *Mandevilla dardanoi* and Their Anti-Inflammatory Activity

Francisca S. V. Lins¹, Thalisson A. de Souza¹, Luiza C. F. Opretzka² , Joanda P. R. e Silva¹, Laiane C. O. Pereira¹, Lucas S. Abreu³ , Anderson A. V. Pinheiro¹, George L. D. dos Santos¹, Yuri M. do Nascimento¹ , José Iranildo Miranda de Melo⁴, Raimundo Braz-Filho⁵ , Cristiane F. Villarreal² , Marcelo S. da Silva¹ and Josean F. Tavares^{1,*} 

¹ Postgraduate Program in Natural and Synthetic Bioactive Products, Federal University of Paraíba, João Pessoa 58051-90, Paraíba, Brazil

² School of Pharmacy, Federal University of Bahia, Salvador 40170-115, Bahia, Brazil

³ Department of Chemistry, Institute of Chemistry, Fluminense Federal University, Niterói 24020-150, Rio de Janeiro, Brazil

⁴ Department of Biology, Centre of Biological Sciences and Health, State University of Paraíba, Campina Grande 58429-500, Paraíba, Brazil

⁵ Department of Chemistry, Institute of Chemistry, Federal Rural University of Rio de Janeiro, Seropédica 23851-970, Rio de Janeiro, Brazil

* Correspondence: josean@lf.ufpb.br



Citation: Lins, F.S.V.; de Souza, T.A.; Opretzka, L.C.F.; e Silva, J.P.R.; Pereira, L.C.O.; Abreu, L.S.; Pinheiro, A.A.V.; dos Santos, G.L.D.; do Nascimento, Y.M.; de Melo, J.I.M.; et al. New Pregnane Glycosides from *Mandevilla dardanoi* and Their Anti-Inflammatory Activity. *Molecules* **2022**, *27*, 5992. <https://doi.org/10.3390/molecules27185992>

Academic Editor: José Carlos Tavares Carvalho

Received: 14 August 2022

Accepted: 9 September 2022

Published: 14 September 2022

Publisher's Note: MDPI stays neutral with regard to jurisdictional claims in published maps and institutional affiliations.



Copyright: © 2022 by the authors. Licensee MDPI, Basel, Switzerland. This article is an open access article distributed under the terms and conditions of the Creative Commons Attribution (CC BY) license (<https://creativecommons.org/licenses/by/4.0/>).

Abstract: *Mandevilla* Lindl. is an important genus of the Apocynaceae family, not only as ornamental plants but also for its medicinal uses. In Brazil, *Mandevilla* species are indicated to treat asthma and skin infections, their anti-inflammatory potential and wound healing properties are also reported in the literature. Concerning their chemical composition, this group of plants is a conspicuous producer of pregnane glycosides. *Mandevilla dardanoi* is an endemic species from the Brazilian semiarid region not studied by any phytochemical methods. In view of the medicinal potential of *Mandevilla* species, this study aimed to isolate new pregnane glycosides from *M. dardanoi*. To achieve this main goal, modern chromatography techniques were employed. Five new pregnane glycosides, dardanols A-E, were isolated from the roots of *M. dardanoi* by HPLC. Their structures were determined using extensive 1D and 2D-NMR and mass spectrometry (MSⁿ and HRESIMS) data. The cytotoxicity and the anti-inflammatory potential of these compounds were evaluated. The first was evaluated by measuring proinflammatory cytokines and nitric oxide production by stimulated macrophages. Dardanols were able to inhibit the production of nitric oxide and reduce IL-1 β and TNF- α . The current work demonstrates the chemodiversity of Brazilian semiarid species and contributes to amplifying knowledge about the biological potential of the *Mandevilla* genus.

Keywords: *Mandevilla dardanoi*; Apocynaceae; pregnane glycosides; anti-inflammatory

1. Introduction

Mandevilla Lindl. is one of the largest neotropical genera of the Apocynaceae family, this group comprises approximately 170 species [1–3]. First registered in 2017, *M. dardanoi* M.F. Sales, Kin.-Gouv. & A.O. Simões is an endemic species from the Brazilian semiarid region, occurring in the states of Pernambuco and Paraíba [4], there are no studies regarding their chemical composition or pharmacological activities [4]. Rich in flavonoids, steroids, and pregnane glycosides *Mandevilla* species have been used by folk medicine in therapy for snakebites, wound healing, and to treat skin infections and inflammation [5–10].

Composed of a steroidal scaffold, the pregnane (C₂₁) and seco-pregnane-type glycosides mainly occur in Apocynaceae, Malpighiaceae, Ranunculaceae, and Zygophyllaceae families [11]. This class of compounds has demonstrated remarkable biological activities, including anticancer, antinociceptive, anti-inflammatory, antiviral, and antibacterial

properties [12–16]. Considering the medicinal potential of *Mandevilla* species, the current study aimed to isolate novel bioactive pregnane derivatives from the roots of *M. dardanoi*. Five new pregnane glycosides, dardanols A–E, were isolated and characterized by spectroscopic and spectrometric analysis. The cytotoxicity and anti-inflammatory activity of dardanols A, B, C, and E were also assessed. All of the compounds tested were active in the models applied.

2. Results and Discussion

2.1. Structural Assignment

Compound **1** was isolated as a white powder with a positive optical rotation of $[\alpha]_D^{25} +14$ (c 0.1, pyridine). Its molecular formula was determined to be $C_{57}H_{90}O_{20}$ by the sodium adduct HRESIMS ion at m/z 1117.5921 $[M + Na]^+$ (calcd. for $C_{57}H_{90}NaO_{20}$, 1117.5917, $\Delta = 0.3$ ppm), indicating 13 indices of hydrogen deficiency (IHD) (Figure S1).

The 1H and ^{13}C NMR data (Tables 1 and 2 and supporting information) showed characteristic signals (chemical shifts given in ppm) of pregnane glycosides already isolated from the *Mandevilla* genus. The hydrogen signals at δ_H 5.75 (d, $J = 2.5$ Hz, H-16) corresponding to an acetal group hydrogen, δ_H 5.41 (m, H-6), an olefinic hydrogen, δ_H 4.58 (t, $J = 2.4$ Hz, H-20) and 3.81 (m, H-3), oxymethinic hydrogens, 1.06 (s, CH_3 -18) and 0.94 (s, CH_3 -19), methyl hydrogens, associated with their respective carbons at δ_C 104.2 (C-16), 122.1 (C-6), 78.9 (C-20), 77.5 (C-3), 16.9 (C-18) and 19.7 (C-19), are in agreement with the values described for the aglycone illustrol, a seco-norpregnane derivative, isolated from *M. illustris* and reported only once [17]. The five anomeric hydrogen signals at 4.76 (dd, $J = 9.5, 2.0$ Hz, H-1'), 5.47 (dd, $J = 4.4, 2.2$ Hz, H-1''), δ_H 5.15 (dd, $J = 9.6, 1.6$ Hz, H-1'''), δ_H 5.08 (dd, $J = 9.6, 1.7$ Hz, H-1''''') and 4.71 (dd, $J = 9.7, 2.0$ Hz, H-1'''''), as well as the presence of the methyl hydrogen signals at 1.49 (3H, d, $J = 6.4$ Hz, C-6'), 1.33 (6H, d, $J = 6.2$ Hz, C-6'' and C-6'''), 1.39 (3H, d, $J = 6.2$ Hz, C-6''''') and 1.29 (3H, d, $J = 6.4$ Hz, C-6'''''), and the hydrogens of the methoxy groups at δ_H 3.33 (s, OCH_3 ''), δ_H 3.39 (s, OCH_3 '''), δ_H 3.60 (s, OCH_3 '''''), δ_H 3.46 (s, OCH_3 '''''''), and δ_H 3.38 (s, OCH_3 ''''''') indicated the existence of five osidic units in the structure of **1**. This evidence was corroborated by the presence of the signals in the ^{13}C NMR spectrum corresponding to five anomeric carbons at δ_C 102.9, 100.9, 100.8, 99.0, and 97.3, five methyl carbons at δ_C 19.0, δ_C 18.9, δ_C 18.4, δ_C 17.5, and δ_C 17.2, and five methoxy carbons at δ_C 59.3, δ_C 58.9, δ_C 56.8, δ_C 56.7, and δ_C 56.5.

In the HSQC spectrum, the anomeric hydrogen at δ_H 4.76 (dd, $J = 9.5, 2.0$ Hz) correlated with the carbon signal at δ_C 99.0. In the HMBC spectrum, this same hydrogen showed a long-distance correlation with the carbon at δ_C 77.6 (C-3), thus being assigned to H-1'. Conversely, the hydrogen signal at δ_H 3.81 (H-3) correlated with the carbon at δ_C 99.0, confirming the bonding of the first glycosyl unit to the aglycone portion. Furthermore, this assignment was corroborated through cross-correlations of δ_H 3.81 (H-3) and δ_H 5.41 (H-6) with δ_C 39.6 (C-4). In the COSY spectrum, a correlation of the signal at δ_H 4.76 (H-1) with δ_H 2.22 (H-2') and of that with δ_H 3.41 (H-3') was observed. In the HSQC spectrum, H-2' and H-3' correlated with the carbons at δ_C 28.7 (C-2') and δ_C 81.3, respectively. These data compared with the literature allowed us to assign the osidic unit I as being diginopyransideo [18]. The H-1' coupling constants at 9.7 and 2.0 Hz are compatible with β -glycosidic bonding. According to the literature, a chemical shift of C-2 of the osidic units smaller than 34 ppm corresponds to an L configuration and larger than 35 ppm to a D configuration [19]. This effect is associated with the orientation of the ether group in the axial present in C-4, which causes a gamma shielding effect at C-2'. Thus, with the chemical shift of C-2' being equal to δ_C 28.7, it was possible to assign the configuration of the osidic unit I as β -L-diginopyranosyl.

Table 1. ¹H NMR spectroscopic data of the sugar moieties of compounds 1–5 (pyridine-*d*₅).

Position	1 ^a	2 ^a	3 ^b	4 ^b	5 ^b
1	1.75; 1.04 (m)	1.74; 1.04 (m)	1.76, 1.05 (m)	1.76; 1.05 (m)	1.76 (m); 1.04 (m)
2	2.04; 1.67 (m)	2.04; 1.68 (m)	2.04, 1.68 (m)	2.08; 1.73 (m)	1.90; 1.65 (m)
3	3.81 (m)	3.83 (m)	3.84 (m)	3.80 (m)	3.81 (m)
4	2.56 (ddd, 13.4, 4.6, 2.2)	2.56 (m)	2.59 (m)	2.36 (ddd, 13.1, 4.8, 2.2);	2.46 (m)
5	2.38 (m)	2.38 (m)	2.38 (m)	2.60 (dd, 13.1, 11.2)	2.36 (m)
6	-	-	-	-	-
7	5.41 (m)	5.42 (m)	5.50 (br s)	5.51 (m)	5.39 (d, 2.84)
8	2.50; 2.28 (m)	2.50; 2.28 (m)	2.64 (m)	2.67 (m)	2.56 (m); 2.30 (m)
9	2.02 (m)	2.02 (m)	2.04 (m)	1.81 (m)	2.05 (m)
10	1.55 (m)	1.57 (m)	1.44 (m)	1.46 (m)	1.55
11	-	-	-	-	-
12	1.45 (m)	1.45 (m)	1.53, 1.30 (m)	1.53, 1.38 (m)	1.65 (m)
13	1.54; 1.44 (m)	1.52; 1.46 (m)	1.95; 1.45 (m)	1.99, 1.45 (m)	2.05 (m); 2.28 (m)
14	-	-	-	-	-
15	-	-	-	-	5.00 (d, 11.5)
16	5.75 (d, 2.5)	5.76 (d, 2.5)	5.17 (s)	5.18 (s)	5.89 (d, 4.4)
17	2.52 (t, 2.7)	2.52 (t, 2.7)	3.23 (d, 8.0)	3.25 (d, 8.0)	2.46 (dd, 4.4, 6.0)
18	1.06 (s)	1.06 (s)	1.40 (s)	1.42 (s)	1.02 (s)
19	0.94 (s)	0.94 (s)	0.95 (s)	0.98 (s)	1.00 (s)
20	4.58 (t, 2.4)	4.58 (m)	5.08 (m)	5.10 (ddd, 8.0, 5.2, 1.2)	4.55 (dd, 3.3, 6.2)
21	4.20 (d, 9.9)	4.21 (d, 9.9)	4.12 (br d, 9.2)	4.23 (dd, 10.1, 1.7)	4.38 (d, 9.7)
MeO-16	3.92 (dd, 9.9, 2.5)	3.93 (dd, 9.9, 2.5)	4.03 (m)	4.05 (dd, 10.1, 5.3)	3.81 (dd, 9.84, 3.48)
OH-14	-	-	3.34 (s)	3.34 (s)	-
	-	-	6.88 (s)	6.90 (s)	-
Osidic units					
A					
1'	4.76 (dd, 9.5, 2.0)	4.78 (dd, 9.5, 2.0)	4.75 (dd, 9.3, 2.2)	4.81 (dd, 11.6, 4.0)	4.74 (dd, 9.5, 2.0)
2'	2.20, 2.13 (m)	2.20, 2.15 (m)	2.16 (m)	2.32 (m); 2.16 (m)	2.20, 2.10
3'	3.41 (m)	3.41 (m)	3.37 (m)	3.43 (ddd, 12.0, 4.6, 2.9)	3.41
4'	3.94 (m)	3.96 (m)	3.97 (br s)	3.90 (m)	3.94
5'	3.56 (qd, 6.4)	3.57 (qd, 6.4)	3.50 (m)	3.56 (dq, 6.5, 1.2)	3.56 (qd, 6.4)
6'	1.49 (d, 6.4)	1.51 (d, 6.4)	1.29 (d, 6.3)	1.55 (d, 6.5)	1.49 (d, 6.4)
MeO	3.33 (s)	3.33 (s)	3.32 (s)	3.40 (s)	3.35 (s)
OH-4'	-	-	-	5.91 (m)	-
B					
1''	5.47 (dd, 4.4, 2.2)	5.40 (dd, 4.4, 2.2)	5.47 (dd, 4.7, 2.6)	-	5.50 (m)
2''	2.21, 2.12 (m)	2.20, 2.12 (m)	2.15 (m)	-	2.18, 2.10
3''	3.96 (m)	3.99 (m)	3.97 (m)	-	3.96
4''	3.73 (m)	3.75 (m)	3.73 (m)	-	3.73 (m)
5''	4.56 (dd, 6.6, 1.3)	4.56 (m)	4.56 (dq, 6.1, 1.7)	-	4.56 (dd, 6.6, 1.3)
6''	1.33 (d, 6.2)	1.34 (d, 6.2)	1.32 (d, 6.1)	-	1.33 (d, 6.2)
MeO	3.39 (s)	3.39 (s)	3.39 (s)	-	3.39 (s)
C					
1'''	5.15 (dd, 9.6, 1.6)	5.15 (dd, 9.6, 1.7)	5.15 (dd, 9.5, 1.9)	-	5.08 (dd, 9.6, 1.6)
2'''	2.30, 1.90	2.38, 1.86 (m)	2.34, 1.87 (m)	-	2.30, 1.90
3'''	4.07 (m)	4.03 (m)	4.05 (m)	-	4.08 (m)
4'''	3.48 (m)	3.52 (m)	3.45 (m)	-	3.48 (m)
5'''	4.16 (m)	4.19 (m)	4.16 (m)	-	4.16 (m)
6'''	1.33 (d, 6.2)	1.39 (d, 6.2)	1.33 (d, 6.1)	-	1.33 (d, 6.2)
MeO	3.60 (s)	3.46 (s)	3.60 (s)	-	3.61 (s)
D					
1''''	5.08 (dd, 9.6, 1.7)	4.71 (dd, 9.7, 2.0)	5.09 (dd, 9.7, 2.2)	-	5.15 (dd, 9.6, 1.7)
2''''	2.38, 1.80 (m)	2.20, 2.05 (m)	2.31, 1.78 (m)	-	2.35, 1.80
3''''	4.01 (m)	3.50 (m)	3.99 (m)	-	4.01 (m)
4''''	3.48 (m)	5.38 (d, 2.9)	3.45 (m)	-	3.48 (m)
5''''	4.17 (m)	3.67 (dq, 6.4, 0.9)	4.16 (m)	-	4.15 (m)
6''''	1.39 (d, 6.2)	1.28 (d, 6.4)	1.38 (d, 6.2)	-	1.39 (d, 6.2)
MeO	3.46 (s)	3.38 (s)	3.46 (s)	-	3.49 (s)
E					
1'''''	4.71 (dd, 9.7, 2.0)	-	4.71 (dd, 9.6, 2.1)	-	4.71 (dd, 9.7, 2.0)
2'''''	2.21, 2.05 (m)	-	2.17, 2.04 (m)	-	2.25, 2.10
3'''''	3.52 (m)	-	3.48 (m)	-	3.52 (m)
4'''''	5.38 (d, 2.9)	-	5.37 (d, 3.0)	-	5.38 (d, 2.9)
5'''''	3.69 (dq, 6.4, 0.9)	-	3.68 (dq, 6.5, 1.2)	-	3.70 (m)
6'''''	1.29 (d, 6.4)	-	1.50 (d, 6.5)	-	1.30 (d, 6.4)
MeO	3.38 (s)	-	3.32 (s)	-	3.41 (s)
Ac	-	-	-	-	-
4''''''	-	2.01 (s)	-	-	-
4''''''	2.02 (s)	-	2.01 (s)	-	2.02 (s)

^a Measured at 500 MHz. ^b Measured at 400 MHz.

Table 2. ^{13}C NMR spectroscopic data of compounds 1–5 (pyridine- d_5).

Position	1 ^a	2 ^a	3 ^b	4 ^b	5 ^b
1	37.1	36.8	37.7	37.7	37.11
2	30.7	30.7	30.5	30.7	30.5
3	77.5	77.6	77.6	77.6	77.4
4	39.8	39.8	39.6	39.7	39.6
5	140.7	140.8	140.2	140.2	140.39
6	122.1	122.2	122.6	122.6	122.28
7	26.0	26.0	26.0	26.0	27.0
8	32.1	32.1	38.9	39.0	34.4
9	46.6	46.7	46.6	46.6	46.5
10	37.4	37.4	37.4	37.4	38.5
11	21.1	21.1	21.9	21.9	19.3
12	30.9	31.0	31.1	31.1	27.2
13	49.1	49.1	46.0	46.0	44.2
14	109.0	109.1	110.1	110.2	87.8
15	-	-	-	-	93.48
16	104.2	104.2	105.8	105.9	109.7
17	56.6	56.7	62.5	62.5	52.9
18	16.9	17.0	20.7	20.7	21.9
19	19.7	19.7	19.7	19.7	19.5
20	78.9	79.0	80.3	80.3	74.7
21	73.9	73.9	71.4	71.4	78.8
MeO-16	-	-	54.4	54.5	-
OH-14	-	-	-	-	-
Osidic units					
A					
1'	99.0	99.0	98.9	99.0	98.9
2'	28.7	28.8	28.6	33.5	28.70
3'	81.4	81.4	81.3	79.5	81.34
4'	71.0	71.0	70.9	67.4	71.02
5'	71.5	71.5	71.4	71.7	71.51
6'	17.5	17.5	17.4	18.0	17.4
MeO	56.5	56.5	56.5	55.6	56.6
B					
1''	97.3	97.3	97.2	-	97.3
2''	33.8	33.9	33.7	-	33.83
3''	76.3	76.4	76.2	-	76.30
4''	78.6	78.6	78.5	-	78.6
5''	63.5	63.6	63.4	-	63.52
6''	18.4	18.4	18.3	-	18.30
MeO	56.8	56.8	56.7	-	56.7
C					
1'''	100.8	-	100.7	-	100.83
2'''	37.0	-	36.9	-	37.03
3'''	78.4	-	78.3	-	78.30
4'''	83.7	-	83.6	-	83.70
5'''	69.4	-	69.5	-	69.5
6'''	18.9	-	18.8	-	18.8
MeO	59.3	-	59.2	-	59.30
D					
1''''	100.9	100.8	100.8	-	100.8
2''''	38.1	38.1	37.0	-	38.1
3''''	78.1	78.2	78.0	-	78.15
4''''	83.6	83.8	83.5	-	83.59
5''''	69.6	69.5	69.3	-	69.58
6''''	19.0	19.0	18.9	-	18.99
MeO	58.9	58.9	58.8	-	58.92
E					
1'''''	102.9	103.0	102.8	-	102.90
2'''''	34.2	34.2	34.1	-	34.20
3'''''	77.4	77.4	77.3	-	77.35
4'''''	68.5	68.5	68.4	-	68.48
5'''''	71.0	71.2	70.0	-	70.1
6'''''	17.2	17.2	17.1	-	17.25
MeO	56.7	56.7	56.5	-	56.65
Ac					
4'''''' a	171.2	171.2	171.1	-	171.1
4'''''' b	21.0	21.2	21.0	-	21.1

^a Measured at 125 MHz. ^b Measured at 100 MHz.

In the HSQC spectrum, the anomeric hydrogen at δ_{H} 5.47 (dd, $J = 4.4$ and 2.2 Hz) correlates with the carbon at δ_{C} 97.3. In the HMBC spectrum, the same signal correlated with the carbon at δ_{C} 71.0 (C-4') was assigned to H-1'', confirming the union of the sugars through 1–4 bonds. In the COSY spectrum, a correlation of the hydrogen H-1'' was observed with the signal at δ_{H} 2.18 and of this with the signal at δ_{H} 3.96, which were assigned to H-2'' and H-3''. In the HSQC spectrum, H-2'' and H-3'' correlate with the carbons at δ_{C} 33.8 and δ_{C} 76.3, respectively. Thus, by comparing the other data that are presented in Table 1 with the data present in the literature, it is possible to assign the osidic unit II as being the sarmentopyranoside [11]. The coupling constants at 4.4 and 2.2 Hz are compatible with α -glycosidic bonding and the C-2'' value at δ_{C} 33.8 with the L configuration for acidic unit II, which was assigned as β -L-sarmentopyranosyl.

In the HSQC spectrum, the anomeric hydrogen at δ_{H} 5.15 (dd, $J = 9.6$ and 1.6 , H-1''') correlated with the carbon at δ_{C} 100.8. In the HMBC spectrum, a correlation of the signal at δ_{H} 3.73 (H-4''') with the carbon at δ_{C} 100.8 was observed, confirming the binding of osidic unit II to III via 1–4 bonds. Similar to assignments performed previously, the COSY and HSQC spectra were analyzed together to perform the ^1H and ^{13}C assignments of osidic unit III (Tables 1 and 2). By comparing these data with the literature, it is possible to assign osidic unit III as a cymaropyranoside [11]. The coupling constants at 9.6 and 1.6 Hz are compatible with β -glycosidic bonding, and the chemical shift value of C-2''' at 37.0 allowed us to assign the configuration of osidic unit III as β -D-cymaropyranosyl.

For osidic unit IV, the signal of the anomeric hydrogen at δ_{H} 5.08 (dd, $J = 9.6$ and 1.7 Hz, H-1''') was observed to correlate in the HSQC spectrum with the carbon at δ_{C} 100.9. In the HMBC spectrum, a correlation of the signal at δ_{H} 3.48 (H-4''') with the carbon at δ_{C} 100.9 was observed, which was assigned to C-1''', confirming the union of osidic units III and IV. In the COSY spectrum, a correlation of δ_{H} 5.08 (H-1''') with δ_{H} 2.35 (H-2''') and of this with δ_{H} 4.01 (H-3''') was observed. In the analysis of the HSQC spectrum, it was possible to assign the respective carbons of the IV osidic units (Table 2). By comparing the data in Tables 1 and 2 with the literature, it was possible to mark osidic unit IV as oleandropyranose [11]. The coupling constant at 9.6 and 1.7 Hz was compatible with β -glycosidic bonding, and the value of C-2''' at δ_{C} 38.1 allowed the assignment of the configuration of osidic unit IV as β -D-oleandropyranosyl.

Finally, anomeric hydrogen was also observed at δ_{H} 4.71 (dd, $J = 9.7$ and 2.0 Hz, H-1''') correlating in the HSQC spectrum with the carbon at δ_{C} 102.9. In HMBC, a correlation of the signal at δ_{H} 3.48 (H-4''') with the carbon at δ_{C} 102 was observed. 9 was observed, confirming the bonding between osidic units IV and V (Figure 1). A correlation of δ_{H} 5.15 (H-1''') with δ_{H} 2.25 (H-2''') was observed in COSY, whose corresponding carbon was signaled by the correlation observed in the HSQC spectrum with the carbon at δ_{C} 34.2 (C-2'''). The other data (Tables 1 and 2) compared with the literature allowed us to assign the glycosidic unit V as simentopyranoside. The coupling constant at 9.7 and 2.0 Hz was compatible with β -glycosidic bonding, and the value of C-2'''' at δ_{C} 34.2 allowed the assignment of the configuration of the osidic unit V as β -L-sarmentopyranosyl. The signal at δ_{H} 5.38 (d, $J = 2.9$ Hz) was assigned to H-4''', whose corresponding carbon was marked at δ_{C} 68.5 by HSQC. In HMBC, a correlation of the signal at δ_{H} 1.29 (d, $J = 6.4$ Hz, 3H-6''') with δ_{C} 68.5 (C-4''') and of δ_{H} 5.38 (H-4''') with the carbon at δ_{C} 171.2 was observed, confirming the position of the acetyl group in osidic unit V at C-4'''' (Figure 2).

After extensive NMR analysis, the structure of **1** was determined to be illustrol-3-O- β -L-diginopyranosyl-(1-4)- α -L-sarmentopyranosyl-(1-4)- β -D-cymaropyranosyl-(1-4)- β -D-oleandropyranosyl-(1-4)- β -L-4-acetoxylsarmentopyranosyl, a new natural product named dar-danol A.

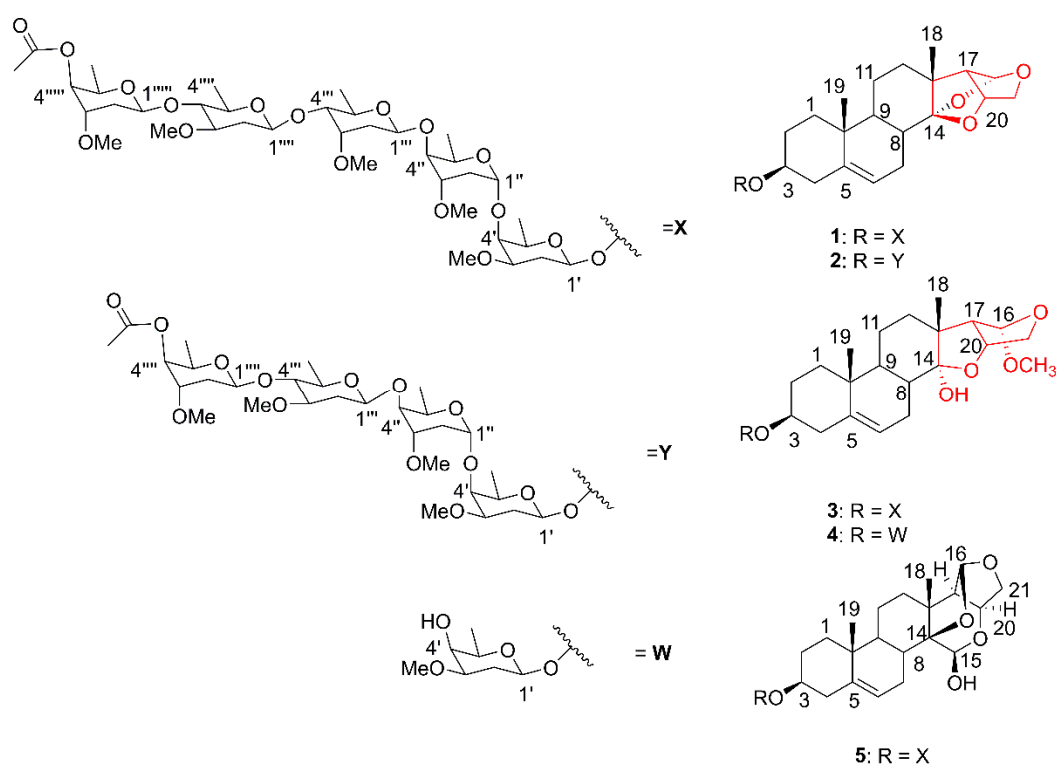


Figure 1. Structures of pregnane glycosides (1–5) isolated from *M. dardanoi*.

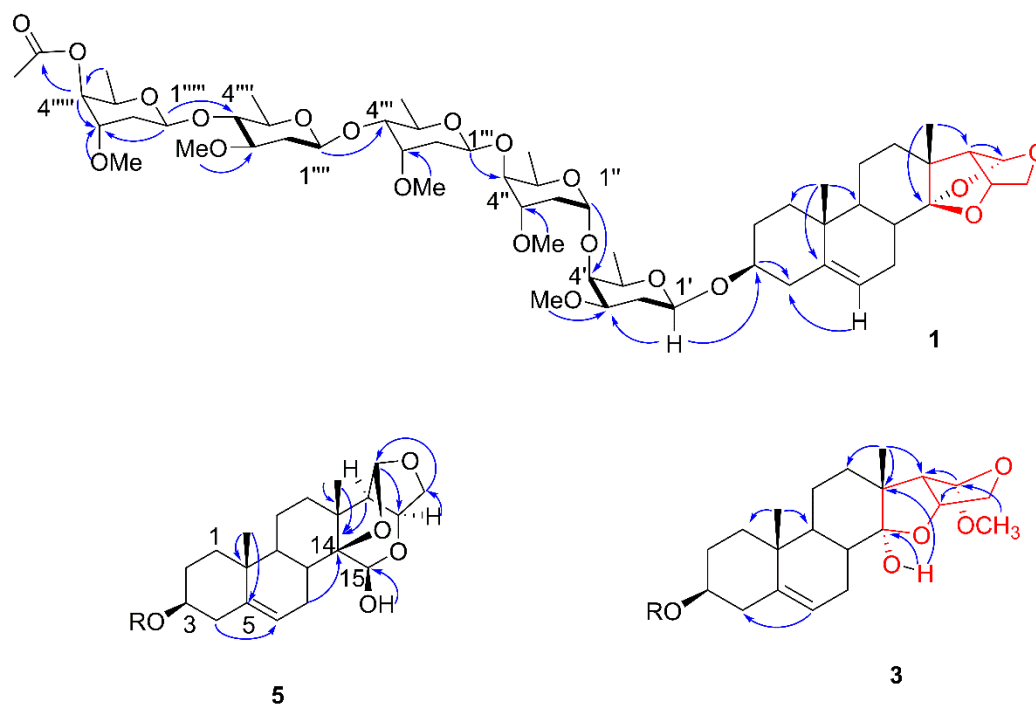


Figure 2. HMBC and COSY correlations of compounds 1, 3 and 5: HMBC and COSY.

Compound 2 was isolated as a white powder with a positive optical rotation of $[\alpha]_D^{25} +18$ (c 0.1, pyridine). Its molecular formula was determined to be $C_{50}H_{78}O_{17}$ by HRESIMS, with m/z 973.5086 $[M + Na]^+$ (calcd for $C_{50}H_{78}NaO_{17}$, 973.5131, $\Delta = 4.7$ ppm), indicating 12 hydrogen deficiency indices. The 1H and ^{13}C NMR data were similar to compound 1 being assigned to illustrol-type aglycone (Tables 1 and 2). When compared to compound 1, a difference of 144 Da was observed in the HRMS spectrum of compound 2, attributed to the absence of a nonterminal osidic unit. This difference can also be visualized

by the presence of the set of signals in the ^1H NMR spectrum, where four anomeric hydrogen signals are visualized at δ_{H} 4.71 (dd, $J = 9.7, 2.0$ Hz), 4.78 (dd, $J = 9.5, 2.0$), 5.15 (dd, $J = 9.6, 1.6$ Hz), and 5.40 (dd, $J = 4.4, 2.2$ Hz), as well as the presence of methyl hydrogen signals at δ_{H} 1.51 (3H, d, $J = 6.4$ Hz, C-6'), 1.34 (3H, d, $J = 6.2$ Hz, C-6''), 1.39 (3H, d, $J = \text{Hz}$, C-6''') and 1.28 (3H, d, $J = 6.2$ Hz, C-6'''), and of the hydrogens of the methoxy groups at δ_{H} 3.33 (s, OCH_3'), δ_{H} 3.39 (s, OCH_3''), δ_{H} 3.46 (s, OCH_3''') and δ_{H} 3.38 (s, OCH_3''''), indicated the existence of four osidic units in compound 2.

The ^1H and ^{13}C NMR data of the osidic units also resembled compound 1, allowing us to establish 2 as illus-trol-3-O- β -L-diginopyranosyl-(1-4)- α -L-sarmentopyranosyl-(1-4)- β -D-cymaropyranosyl-(1-4)- β -L-4-acetoxy-sarmentopyranosyl, a new natural product named dardanol B.

Compound 3 was isolated as a white powder with a positive optical rotation of $[\alpha]_{\text{D}}^{25} +13$ (c 0.1, pyridine). Its molecular formula was determined to be $\text{C}_{58}\text{H}_{94}\text{O}_{21}$ by HRESIMS, with m/z 1109.6252 $[\text{M} - \text{H}_2\text{O} + \text{H}]^+$ (calcd for $\text{C}_{58}\text{H}_{93}\text{O}_{20}$, 1109.6254, $\Delta = 1.0$ ppm), indicating 12 hydrogen deficiency indices. The NMR data resembled that of the aglycone illustrol; however, some differences were observed for the carbons at δ_{C} 38.9, 46 and 62.5, assigned to C-8, C-13 and C-17, respectively, with C-8 and C-17 being deprotected and C-13 protected when compared to the chemical shifts of these carbons in compound 1. These data were associated with one lower hydrogen deficiency index compared with compound 1, suggesting the opening of the C-14-O-C-16 epoxide. The signal at δ_{H} 6.88 (s), uncorrelated in the HSQC spectrum, was assigned to the OH located at C-14. This signal showed correlations in the HMBC spectrum with the signals at δ_{C} 46.0 and 110.1 that were assigned to C-13 and C-14, respectively. Additionally, in the HMBC spectrum, we observed correlations of the signal at δ_{H} 1.40 (3H-18) with the carbons at δ_{C} 110.1 (C-14) and in the HMBC spectrum at δ_{C} 46.0 (C-13) and with δ_{C} 62.5, which was assigned to C-17. The signal at δ_{H} 5.17, whose corresponding carbon in the HSQC spectrum was δ_{C} 105.8, was assigned to C-16. The signal at δ_{H} 5.17 correlated with δ_{C} 46.0 (C-13) and with δ_{C} 62.5 (C-17). A correlation of this signal with δ_{C} 71.4, assigned to C-21, was also observed. A correlation was also observed with the signal at δ_{C} 54.5 that was assigned to methoxy bound at position 16. The coupling constant of H-17 (d, $J = 8.0$) and a singlet for H-16 demonstrated near 90-degree angulation between these hydrogens, and thus, the aglycone was defined as shown in Figure 1. As far as we have searched, no records were found for this type of aglycone. The NMR data (Tables 1 and 2), together with literature data, comparisons with compound 1 data and high-resolution mass spectrometry confirmed the presence of five 1–4 bonded osidic units identical to compound 1 and inserted in C-3 (Table 2).

To reject the possibility that the aglycone had been formed in the process of separating the compounds, a direct infusion on the ESIMS/MS was performed with the crude ethanolic extract. The presence of the ion at m/z 1144.44 $[\text{M} + \text{NH}_4]^+$ was identified, corresponding to compound 3 (Figure 1). Thus, compound 3 was identified as seco-illustrol-3-O- β -L-diginopyranosyl-(1-4)- α -L-sarmentopyranosyl-(1-4)- β -D-cymaropyranosyl-(1-4)- β -D-olean dropyranosyl-(1-4)- β -L-4-acetoxy-sarmentopyranosyl, a new natural product named dardanol C.

Compound 4 was isolated as a white powder with a positive optical rotation of $[\alpha]_{\text{D}}^{25} +17$ (c 0.1, pyridine). Its molecular formula was determined to be $\text{C}_{28}\text{H}_{44}\text{O}_8$ by HRESIMS, m/z 531,2923 $[\text{M} + \text{Na}]^+$ (calcd for $\text{C}_{28}\text{H}_{44}\text{NaO}_8$, 531,2928, $\Delta = 4.2$ ppm), indicating 7 hydrogen deficiency indices. The NMR data for the aglycone of this compound were similar to compound 3, and it could be concluded that it was of the same type as OH at C-14 and OCH_3 at C-16. In the ^{13}C NMR spectrum, it was possible to observe six carbons at δ_{C} 99.0, 33.2, 79.4, 67.4, 71.4 and 20.4 in addition to a signal for methoxyl at δ_{C} 55.3 compared with the literature, and the other osidic units of compounds 1–3 were marked as diginopyranose. The H-1' coupling constant at 11.6 and 4.0 Hz was compatible with β -glycosidic bonding, and the C-2' value at δ_{C} 33.5 allowed the configuration of the osidic unit to be assigned as L-diginopyranosyl. The molecular mass of this compound was also

found in the analysis of the crude extract by ESIMS/MS, which again rejected the possibility of artifacts. Thus, compound **4** was identified as seco-illustrol-3-O- β -L-diginopyranosyl, a new natural product named dardanol D.

Compound **5** was isolated as a white powder with a positive optical rotation of $[\alpha]^{25}_D -19$ (c 0.1, pyridine). Its molecular formula was determined to be $C_{58}H_{92}O_{21}$ by HRESIMS, with m/z 1147.6037 $[M + Na]^+$ (calcd for $C_{57}H_{90}NaO_{20}$, 1147.6023, $\Delta = 4.8$ ppm indicating 13 indices of hydrogen deficiency). The 1H and ^{13}C NMR data showed signals characteristic of pregnane glycosides. The hydrogen signals at δ_H 5.00 (d, $J = 11.5$ Hz), 5.89 (d, $J = 4.4$ Hz) and 4.55 (dd, $J = 6.2, 3.3$ Hz) together with carbons at δ_C 93.5, 109.7 and 74.7 are in agreement with the values described for the velutinol aglycon, reported only in *M. velutinus* [20]. In the RMN 1H spectrum, it was possible to observe five signals for anomeric hydrogens at δ_H 4.74 (dd, $J = 9.5, 2.0$ Hz), 5.50 (m), 5.08 (dd, $J = 9.6, 1.6$ Hz), 5.15 (dd, $J = 9.6, 1.7$ Hz) and 4.71 (dd, $J = 9.7, 2.0$ Hz). These data, compared with compound **1** (Tables 1 and 2), allowed us to assign the same glycosidic units, with the same sequence of inter-unit bonds and the same configuration. Thus, compound **5** was determined as velutinol-3-O- β -L-diginopyranosyl-(1-4)- α -L-sarmentopyranosyl-(1-4)- β -D-cymaropyranosyl-(1-4)- β -D-oleandropyranosyl-(1-4)- β -L-4-acetoxylsarmentopyranosyl, named dardanol E.

2.2. Biological Activity

To assess the anti-inflammatory potential of compounds, J774 macrophages were used as an in vitro model. Macrophages play a key role in inflammation and immune regulation processes, contributing to tissue homeostasis [21,22]. They are tissue-resident or infiltrated immune cells activated upon stimulation of a great number of pro-inflammatory mediators, such as chemokines, cytokines, and nitric oxide (NO) [21]. Here, the nitric oxide production by macrophages stimulated with Lipopolysaccharides (LPS) and Interferon gamma (IFN- γ) was assessed. Stimulated macrophage that received vehicle as treatment (control group) show an increase in NO levels in comparison to non-stimulated macrophages (basal group, $p < 0.01$; Figure 3A–D). The treatment with all the test compounds inhibited the nitric oxide production at a concentration of 200 μ M in comparison to vehicle-treated stimulated cells (Figure 3A–D). Interestingly, the compounds presented different profiles of inhibition. Compound **2** reduced the amount of NO on the supernatant of stimulated cells only at the concentration of 200 μ M (Figure 3B; $p < 0.01$), meanwhile compound **1** exhibited a dose-dependent effect at 200 and 100 μ M (Figure 3A; $p < 0.01$). Plus, compounds **3** and **5** were able to lower the production of NO at the range of 200 μ M to 50 μ M (Figures 1D and 3C, respectively; $p < 0.01$), in a dose-dependent manner. Dexamethasone (20 μ M), the gold-standard drug, was also able to reduce the levels of NO when compared to untreated cells, as expected (Figure 3A–D; $p < 0.001$). Remarkably, at the concentration of 200 μ M compounds **5** and **1** showed greater efficacy in comparison to dexamethasone ($p < 0.05$), while **2** and **3** exhibited a similar efficacy to that of dexamethasone ($p < 0.05$). Importantly, cell toxicity assays (Figure S86; Supplementary Material) show that there was no reduction in cellular viability. These data corroborate the interpretation of the NO assay results, as the decrease of cellular viability could reduce the production of inflammatory mediators, and it could be wrongly acknowledged as anti-inflammatory activity. NO has a ubiquitous role in the maintenance of homeostasis, but upon inflammatory stimuli, it will have mainly a pro-inflammatory role. During the inflammatory response, it will act as an oxidant agent or a signaling mediator, by activating cascades that lead to the production of more inflammatory mediators [23]. Therefore, the ability to reduce the production of this mediator during inflammation is an interesting feature for anti-inflammatory compounds.

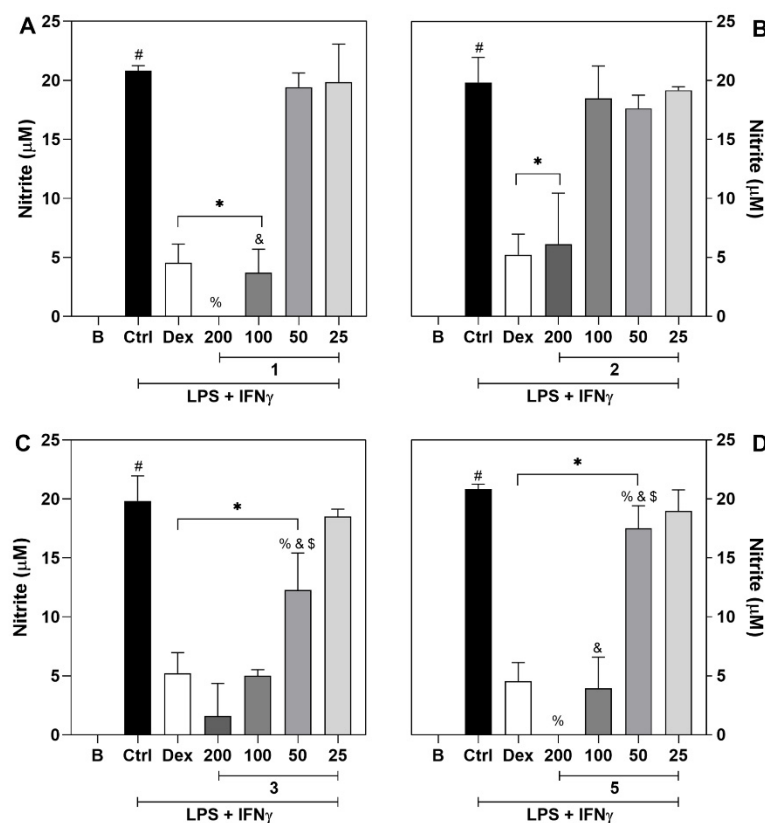


Figure 3. Inhibitory effect of **1**, **2**, **3** and **5** on the production of nitric oxide by stimulated J774 macrophages. Panels (A–D) show nitrite levels determined by the Griess method, of compounds **1** to **5**, respectively. Different concentrations of **1**, **2**, **3** and **5** (25 to 200 µM) or dexamethasone (Dex; 20 µM, reference drug) were added to J774 macrophages cultures in the presence of LPS (500 ng/mL) + IFN- γ (5 ng/mL). Nitrite quantifications were performed 24 h after treatments. The control group (Ctrl) represents vehicle treated cells stimulated with LPS + IFN- γ . The basal group (B) shows data from untreated and unstimulated cells. # Different from the unstimulated (B) group ($p < 0.05$). * Different from the control (Ctrl) group ($p < 0.01$). % Different from the Dex group ($p < 0.05$). & Difference from the 200 µM group ($p < 0.05$). \$ Difference from the 100 µM group ($p < 0.05$).

The modulatory effect of **1**, **2**, **3** and **5** on the pro-inflammatory cytokine production by stimulated macrophages was further assessed. The untreated cells stimulated with LPS and IFN- γ (control group) show an increase in Tumor necrosis factor alpha (TNF- α) and Interleukin 1 beta (IL-1 β) levels in comparison to non-stimulated macrophage (basal group, $p < 0.01$; Figure 4A–H).

Treatment with all tested concentrations (25–200 µM) of the tested compounds resulted in inhibition of TNF- α production (Figure 4A–D, $p < 0.01$). Within the tested range, most of the molecules showed a dose-dependent effect, except for compound **2** which did not show any difference in the magnitude of its effect among the tested concentrations. Dexamethasone, the gold standard drug, also inhibited the production of TNF- α . Importantly, the effect of compounds **1**, **2**, **3** and **5** (Figure 4A; $p < 0.01$) was comparable to that of dexamethasone.

The production of IL-1 β was also modulated by the tested compounds (Figure 4E–H). Compounds **1**, **3** and **5** and **1** on the other hand, display a similar profile. These compounds decrease the amount of IL-1 β at concentrations of 200 and 100 µM (Figure 4E–H, $p < 0.01$) in a similar magnitude to that of dexamethasone but did not show any dose-dependency. Similar but not the same, compound **2** inhibited the production of IL-1 β at concentrations of 200 and 100 µM (Figure 4F, $p < 0.01$), and showed a dose-dependent profile with an effect similar to dexamethasone.

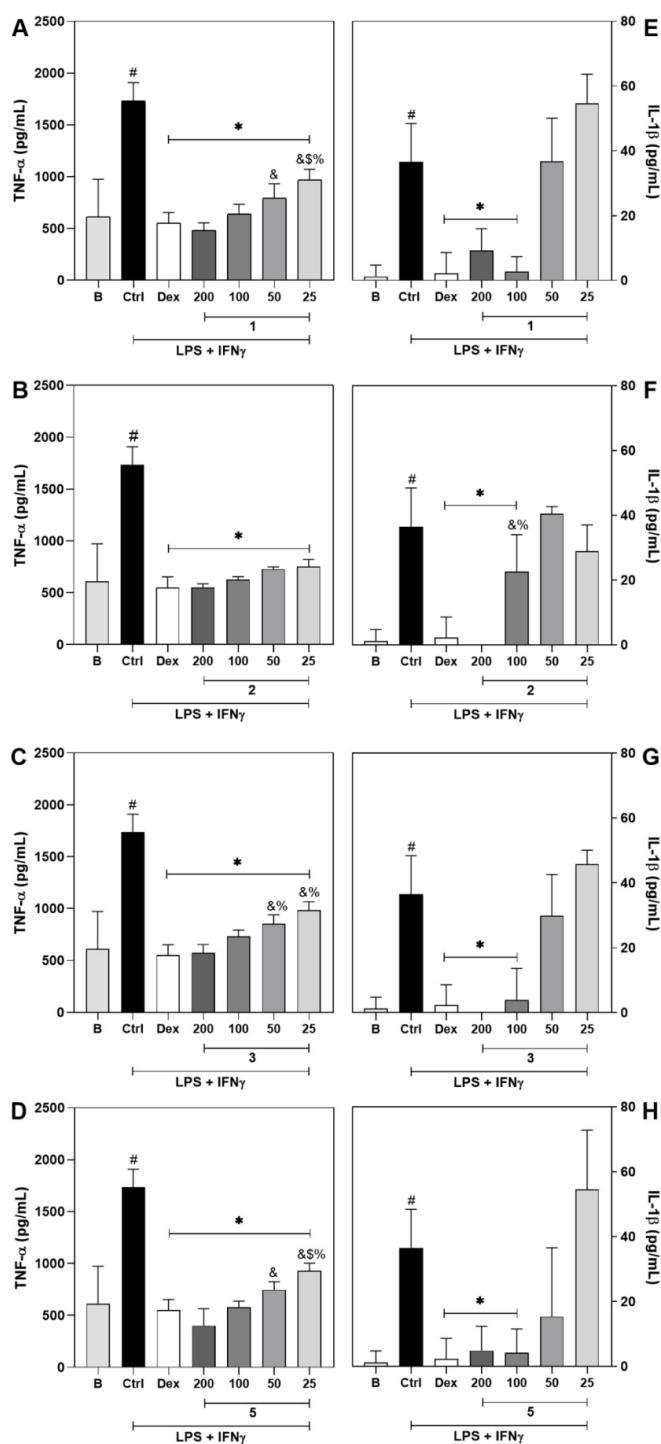


Figure 4. Compounds 1, 2, 3 and 5 exhibit a modulatory effect on the production of TNF- α and IL-1 β in stimulated J774 macrophages. Panels (A–D) show the effect of treatment with 1, 2, 3 or 5 respectively, on TNF- α levels, measured by ELISA. Panels (E–H) show the effect of treatment with 1, 2, 3 or 5 respectively, on IL-1 β levels, measured by ELISA. Different concentrations of 1, 2, 3 and 5 (25–200 μ M) or dexamethasone (Dex; 20 μ M, reference drug) were added to J774 macrophage cultures stimulated with LPS + IFN- γ . The control group (CTRL) represents untreated cells stimulated with LPS + IFN- γ . The basal group (B) shows data from untreated and unstimulated cells. TNF- α and IL-1 β levels were determined 4 h and 24 h after treatments, respectively. # Different from the unstimulated (B) group ($p < 0.05$). * Different from the control (Ctrl) group ($p < 0.01$). % Different from the Dex group ($p < 0.05$). & Difference from the 200 μ M group ($p < 0.05$). \$ Difference from the 100 μ M group ($p < 0.05$).

Together with NO, TNF- α and IL-1 β are important mediators of the inflammatory response. TNF- α is a pro-inflammatory cytokine produced primarily by monocytes/macrophages and it plays a key role in the modulation of immune responses and induction of inflammation. Upon activation of its receptor, a cascade of events leading to the production of more pro-inflammatory mediators is initiated [24]. Moreover, TNF- α is a target to treat several inflammatory diseases, such as rheumatoid arthritis, inflammatory bowel diseases, ankylosing spondylitis, and psoriasis [25]. Similarly, IL-1 β is also recognized as an important cytokine for inflammatory events. It is primarily a pro-inflammatory cytokine capable of inducing its own production, in a positive feedback loop that amplifies the inflammatory signaling [26]. Plus, the enhanced secretion of IL-1 β has been associated with the pathogenesis of autoinflammatory diseases, metabolic syndromes, acute inflammation, chronic inflammation, and malignancy [27].

Therefore, the ability of **1**, **2**, **3** and **5** to reduce the production/release of IL-1 β and TNF- α reinforces the potential anti-inflammatory activity previously displayed by reducing the amount of NO released by stimulated macrophages. Interestingly, velutinol A, an aglycone steroid compound with a structure similar to the tested compounds, was reported to inhibit kinin B1 receptor-mediated inflammatory responses in vivo [28]. Kinin B1 receptor is an inducible receptor that has been implicated in the process of stimulation and release of IL-1 β and TNF- α from macrophages [29].

Data presented here demonstrate that compounds **1**, **2**, **3** and **5** inhibit the production/release of pro-inflammatory mediators, which is an important attribute of anti-inflammatory compounds. Moreover, the tested compounds show a similar or even greater efficacy in comparison to that of dexamethasone, considered the gold-standard drug in the tests. Therefore, these results evidence the anti-inflammatory potential of these compounds.

3. Materials and Methods

3.1. General Information

Sephadex LH-20 gel (Merck, Kenilworth, NJ, USA) and commercial octadecylsilane functionalized silica cartridges ISOLUTE[®] C₁₈ (EC) 500 mg/6 mL were used in the pre-purification of the compounds.

The analytical-scale high-performance liquid chromatographic (HPLC) analyses were performed on a Shimadzu Prominence chromatograph, (flow rate of 600 $\mu\text{L}\cdot\text{min}^{-1}$) and injections of 20 μL , using a reversed-phase analytical column (YMC, 250 \times 4.6 mm and particle size of 5 μC_{18}). The preparative HPLC analysis was used on Shimadzu Proeminence equipment and reverse phase column (YMC, 250 \times 21.2mm and particle size of 5 μC_{18}). The solvents used were acetonitrile (HPLC grade, Tedia[®], Cincinnati, OH, USA) and ultrapure water obtained with a Milli-Q (Millipore[®]).

1D and 2D NMR experiments were performed using Bruker Avance III HD (400 and 100 MHz for ¹H and ¹³C, respectively) and Varian NMR (500 and 125 MHz for ¹H and ¹³C, respectively) spectrometers. The residual peaks of the deuterated solvents were taken as reference points and chemical shifts were given in ppm. Mass spectrometry analyses were performed on an HRMS microTOFII ESI-TOF.

A HPLC Shimadzu (Kyoto, Japan) coupled with an Amazon X (Bruker Daltonics, Billerica, MA, USA) with an electrospray ion (ESI) source, was used to perform ESI-MSn. The analysis parameters were as follows: capillary 4.5 kV, ESI (positive mode for samples from the chloroform phase and negative mode for samples from the ethyl acetate phase), final plate offset 500 V, 40 psi nebulizer, dry gas (N₂) with a flow rate of 8 mL/min and a temperature of 200 °C. Collision-induced dissociation (CID) fragmentation was achieved in the Amazon X in auto-MS/MS mode using the enhanced resolution mode. The mass spectra (m/z 50–1300) were recorded every 2 s. Moreover, these samples were injected again into an HPLC system coupled to a microTOF II mass spectrometer (Bruker Daltonics, Billerica, MA, USA) for high resolution electrospray ionization mass spectrometry (HRESIMS) analyses using the same method as previously reported [30].

3.2. Plant Material

The roots of *M. dardanoi* were collected at Serra do Jatobá (07°29'00'' S, 36°39'54'' O), located in Serra Branca, Paraíba, Brazil. The botanical material was identified by Prof. Dr. José Iranildo Miranda de Melo, from the Department of Biology, Centre of Biological Sciences and Health of the Paraíba State University (UEPB), and later deposited in the Herbarium Manuel de Arruda Câmara (HACAM-UEPB), where a voucher was produced, number 1663. Access registration in the National System for the Management of Genetic Heritage and Associated Traditional Knowledge (SISGEN) was obtained under code A5B0BFC.

3.3. Extraction and Isolation

The roots of *M. dardanoi* were dried in a circulating air oven at 45 °C for 92 h and then ground in a knife mill, obtaining 1.78 kg of powder. This material was macerated with 95% ethanol for 72 h in five repetitions and the extracted solution was concentrated in a rotary evaporator (40 °C), resulting in 303 g of the crude ethanolic extract (BSE-Md). Subsequently, 290 g of the BSE-Md was solubilized in MeOH/H₂O (7:3, v/v). This solution was subjected to partitioning with solvents of an increasing degree of polarity (using 2 L of each solvent: hexane, chloroform, ethyl acetate, and n-butanol). The partitioning allowed obtaining the following phases: hexane (18.2 g), chloroform (12 g), ethyl acetate (4.2 g), and n-butanol (15 g).

For fractionation of the chloroform phase, 3 g were submitted to Sephadex LH-20 gel permeation chromatography, with isocratic elution (MeOH). This method allowed the isolation of 10 fractions (Md-S1 to Md-S10), which were analyzed by CCD. The fractions Md-S1-Md-S5 were subjected to reversed-phase chromatography (C18), with gradient elution using MeOH/H₂O (7:3 v/v), 20 fractions were obtained (Md-C18.1-Md-C18.20). Of these, fractions Md-C18.1 to Md-C18.6 (MeOH/H₂O 8:2 v/v) were pooled, yielding 360 mg, subsequently, this fraction was subjected to preparative HPLC.

In the preparative HPLC analysis mobile phase was composed by binary mixture of water and acetonitrile (70:30, v/v), through the isocratic elution mode, with a flow rate of 8.0 mL/min, for 80 min. The wavelength used was 205 nm, obtaining in the end 23 fractions. The fractions Md-235-21, Md-235-15, Md-235-16, Md-235-04 and Md-235-18, after undergoing structural elucidation techniques, provided compounds **1** (3.2 mg, $t_R = 53.81$ min), **2** (1.8 mg, $t_R = 37.80$ min), **3** (2.2 mg, $t_R = 39.48$ min), **4** (1.2 mg, $t_R = 12.18$ min) and **5** (1.6 mg, $t_R = 46.95$ min), respectively.

Nuclear magnetic resonance (NMR) spectra were obtained using spectrometer Bruker 400 MHz (¹H) and 100 MHz (¹³C) and Varian NMR (500 and 125 MHz for ¹H and ¹³C, respectively) at the Center of Characterization and Analysis of the Federal University of Paraíba. Deuterated solvent (pyridine-*d*₅ (C₅D₅N) was used in the solubilization of the samples for NMR and chemical shifts (δ) were recorded in ppm (parts per million) and coupling constants (*J*) in Hz.

3.4. Cytotoxicity to Mammalian Cells

To determine the cytotoxicity of **1**, **2**, **3** and **5**, murine macrophage-like J774 cells were plated into 96-well plates at a cell density of 2×10^5 cells/well in Dulbecco's modified Eagle medium (DMEM; Life Technologies, GIBCO-BRL, Gaithersburg, MD) supplemented with 10% fetal bovine serum (FBS; GIBCO, Invitrogen, Dun Laoghaire, Ireland) and 50 µg/mL of gentamycin (Novafarma, Anápolis, GO, Brazil), and incubated for 24 h at 37 °C and 5% CO₂, as previously described [31]. The cells were then stimulated with LPS (500 ng/mL, Sigma Chemical Co., St. Louis, MO, USA) and IFN- γ (5 ng/mL, Sigma). The compounds **1**, **2**, **3** or **5** were added to the medium at five concentrations ranging from 25 to 200 µM in triplicate and incubated for 72 h. After, 20 µL/well of Alamar Blue (Invitrogen, Carlsbad, CA, USA) was added to the plates for 6h. Colorimetric readings were performed at 570 and 600 nm. Gentian violet (Synth, São Paulo, Brazil) at 10 µM was used as the positive control.

3.5. Assessment of Cytokine and Nitric Oxide Production by Macrophages

For cytokine and nitric oxide evaluations, J774 cells were seeded in 96-well tissue culture plates at 2×10^5 cells/well in DMEM medium supplemented with 10% of FBS and 50 $\mu\text{g}/\text{mL}$ of gentamycin for 2 h at 37 °C and 5% CO_2 , as described previously [32]. Cells were then stimulated with LPS (500 ng/mL) and IFN- γ (5 ng/mL) in the presence of 1, 2, 3 or 5 at different concentrations (25 to 200 μM), medium (control group), or dexamethasone (20 μM , gold-standard drug), and incubated at 37 °C. Cell-free supernatants were collected 4 h after the incubation for TNF- α quantification, or 24 h after the incubation for IL-1 β and nitrite quantification. Cytokine concentrations in supernatants from J774 cultures were determined by enzyme-linked immunosorbent assay (ELISA), using the DuoSet kit from R&D Systems (Minneapolis, MN), according to the manufacturer's instructions. The results were expressed in picograms/mL of IL-1 β . Quantification of nitrite as an indicator of nitric oxide production was performed using the Griess method [33].

3.6. Statistical Analysis

Data are presented as mean \pm standard deviation (SD) of 3 replicates. Comparisons between groups were made using one-way ANOVA with Tukey post-hoc test. Analyses were performed using Prism 8 Computer Software (GraphPad, San Diego, CA, USA), with a statistical significance of $p < 0.05$.

3.7. Characterization

Dardanol A (1): white powder; $[\alpha]^{25}_{\text{D}} + 14$ (c 0.1, pyridine); ^1H and ^{13}C NMR data, see Tables 1 and 2; positive-ion HRESIMS m/z 1117.5918 $[\text{M} + \text{Na}]^+$ (calcd for $\text{C}_{57}\text{H}_{90}\text{NaO}_{20}$, 1117.5917).

Dardanol B (2): white powder; $[\alpha]^{25}_{\text{D}} + 18$ (c 0.1, pyridine); ^1H and ^{13}C NMR data, see Tables 1 and 2; positive-ion HRESIMS m/z 973.5086 $[\text{M} + \text{Na}]^+$ (calcd for $\text{C}_{50}\text{H}_{78}\text{NaO}_{17}$, 973.5131).

Dardanol C (3): white powder; $[\alpha]^{25}_{\text{D}} + 13$ (c 0.1, pyridine); ^1H and ^{13}C NMR data, see Tables 1 and 2; positive-ion HRESIMS m/z 1109.6252 $[\text{M} - \text{H}_2\text{O} + \text{H}]^+$ (calcd for $\text{C}_{58}\text{H}_{93}\text{O}_{20}$, 1109.6254).

Dardanol D (4): white powder; $[\alpha]^{25}_{\text{D}} + 17$ (c 0.1, pyridine); ^1H and ^{13}C NMR data, see Tables 1 and 2; positive-ion HRESIMS m/z 531.2923 $[\text{M} + \text{Na}]^+$ (calcd for $\text{C}_{28}\text{H}_{44}\text{NaO}_8$, 531.2928).

Dardanol E (5): white powder; $[\alpha]^{25}_{\text{D}} - 19$ (c 0.1, pyridine); ^1H and ^{13}C NMR data, see Tables 1 and 2; positive-ion HRESIMS m/z 1147.6037 $[\text{M} + \text{Na}]^+$ (calcd for $\text{C}_{57}\text{H}_{90}\text{NaO}_{20}$, 1147.6023).

4. Conclusions

Five new pregnane steroidal glycosides (dardanols A–E) were isolated from the ethanolic extract of *Mandevilla dardanoi* by modern chromatographic techniques and characterized by comprehensive spectroscopic data. Among them, compounds 3 and 4 contained a novel seco-pregnane-type aglycone. Dardanols A, B, C and E showed anti-inflammatory potential by inhibiting the production of nitric oxide and reducing the pro-inflammatory cytokines IL-1 β and

TNF- α in stimulated macrophages. These findings enrich the knowledge of the chemodiversity and biological potential of Caatinga species.

Supplementary Materials: The following supporting information can be downloaded at: <https://www.mdpi.com/article/10.3390/molecules27185992/s1>, Figure S1: ESI-HRMS spectrum of compound 1; Figure S2: ^1H NMR spectrum (500 MHz, pyridine- d_5) of compound 1; Figures S3–S6: Expansion of ^1H NMR spectrum (500 MHz, pyridine- d_5) of compound 1; Figure S7: APT NMR spectrum (125 MHz, pyridine- d_5) of compound 1; Figures S8–S10: Expansion APT NMR spectrum (125 MHz, pyridine- d_5) of compound 1; Figure S11: HSQC spectrum(500 and 125 MHz, pyridine- d_5) of compound 1; Figures S12–S15: Expansion of HSQC spectrum(500 and 125 MHz, pyridine- d_5) of compound 1; Figure S16: HMBC spectrum(500 and 125 MHz, pyridine- d_5) of compound 1; Figure S17–S19: Expansion of HMBC spectrum(500 and 125 MHz, pyridine- d_5) of compound 1; Figure S20: COSY spectrum (500 MHz, pyridine- d_5)of compound 1; Figure S21: NOESY spectrum (500 MHz, pyridine- d_5) of compound 1; Figure S22: TOCSY spectrum (500 MHz, pyridine- d_5) of compound 1; Figure S23: ESI-HRMS spectrum of compound 2; Figure S24: ^1H NMR spectrum (500 MHz, pyridine- d_5) of compound 2; Figures S25–S27: Expansion of ^1H NMR spectrum (500 MHz, pyridine- d_5) of compound 2; Figure S28: Dept 135 NMR spectrum (500 MHz, pyridine- d_5)of compound 2; Figures S29–S30: Expansion of Dept 135 NMR spectrum (125 MHz, pyridine- d_5) of compound 2; Figure S31: HSQC spectrum(500 and 125 MHz, pyridine- d_5 ,) of compound 2; Figures S32–S33: Expansion of HSQC spectrum(500 and 125 MHz, pyridine- d_5) of compound 2; Figure S34: HMBC spectrum(500 and 125 MHz, pyridine- d_5) of compound 2; Figures S35–S36: Expansion of HMBC spectrum(500 and 125 MHz, pyridine- d_5) of compound 2; Figure S37: COSY spectrum (500 MHz, pyridine- d_5) of compound 2; Figure S38: ESI-HRMS spectrum of compound 3; Figure S39: ^1H NMR spectrum (400 MHz, pyridine- d_5) of compound 3; Figure S40–S42: Expansion of ^1H NMR spectrum (400 MHz, pyridine- d_5) of compound 3; Figure S43: APT NMR spectrum (400 MHz, pyridine- d_5) of compound 3; Figure S44–S45: Expansion of APT NMR spectrum (400 MHz, pyridine- d_5) of compound 3; Figure S46: HSQC spectrum(400 MHz, pyridine- d_5) of compound 3; Figures S47–S50: Expansion of HSQC spectrum(400 and 100 MHz, pyridine- d_5) of compound 3; Figure S51: HMBC spectrum(400 and 100 MHz, pyridine- d_5) of compound 3; Figure S52: Expansion of HMBC spectrum(400 and 100 MHz, pyridine- d_5) of compound 3; Figure S53: HMBC spectrum(400 and 100 MHz, pyridine- d_5) of compound 3; Figure S54: COSY NMR spectrum (400 MHz, pyridine- d_5) of compound 3; Figure S55: ESI-HRMS spectrum of compound 4; Figure S56: ^1H NMR spectrum (400 MHz, pyridine- d_5) of compound 4; Figure S57: Expansion of ^1H NMR spectrum (400 MHz, pyridine- d_5) of compound 4; Figures S58–S59: ^1H NMR spectrum (400 MHz, pyridine- d_5) of compound 4; Figure S60: ^{13}C NMR spectrum (100 MHz, pyridine- d_5) of compound 4; Figure S61: DEPT 135 spectrum (100 MHz, pyridine- d_5) of compound 4; Figure S62: Expansion of DEPT 135 spectrum (100 MHz, pyridine- d_5) of compound 4; Figure S63: HSQC spectrum (400 and 100 MHz, pyridine- d_5) of compound 4; Figures S64–S65: Expansion of HSQC spectrum (400 and 100 MHz, pyridine- d_5) of compound 4; Figure S66: HMBC spectrum (400 and 100 MHz, pyridine- d_5) of compound 4; Figure S67: Expansion of HMBC spectrum (400 and 100 MHz, pyridine- d_5) of compound 4; Figure S68: HMBC spectrum (400 and 100 MHz, pyridine- d_5) of compound 4; Figure S69: COSY spectrum (400 MHz, pyridine- d_5) of compound 4; Figure S70: ESI-HRMS spectrum of compound 5; Figure S71: ^1H NMR spectrum (400 MHz, pyridine- d_5) of compound 5; Figures S72–S73: Expansion of ^1H NMR spectrum (400 MHz, pyridine- d_5) of compound 5; Figure S74: ^{13}C NMR spectrum (100 MHz, pyridine- d_5) of compound 5; Figures S75–S76: Expansion of ^{13}C NMR spectrum (100 MHz, pyridine- d_5)of compound 5; Figure S77: DEPT 135 spectrum of compound 5; Figure S78: DEPT 135 spectrum (100 MHz, pyridine- d_5)of compound 5; Figures S79–S81: HSQC spectrum (400 and 100 MHz, pyridine- d_5) of compound 5; Figure S82: HMBC spectrum (400 and 100 MHz, pyridine- d_5) of compound 5; Figures S83–S84: Expansion of HMBC spectrum (400 and 100 MHz, pyridine- d_5) of compound 5; Figure S85: COSY spectrum (400 MHz, pyridine- d_5) of compound 5; Figure S86: Effect of 1, 2, 3 and 5 on cell viability of stimulated J774 macrophages.

Author Contributions: Plant material identification, J.I.M.d.M.; chemical methods, F.S.V.L., J.P.R.e.S., L.C.O.P., L.S.A., T.A.d.S., A.A.V.P., G.L.D.d.S. and Y.M.d.N.; biological assay and interpretation data, L.C.F.O. and C.F.V.; data analysis and structural elucidation, L.S.A., T.A.d.S., R.B.-F., M.S.d.S., J.F.T. All authors have read and agreed to the published version of the manuscript.

Funding: This research was funded by Brazilian agencies; Coordenação de Aperfeiçoamento de Pessoal de Nível Superior-Brasil (CAPES) (Finance Code 001), Conselho Nacional de Desenvolvimento Científico e Tecnológico (CNPq Finance Code 465536/2014-0) and FINEP by means of Rede Norte-Nordeste de Fitoterápicos (INCT-RENNOFITO).

Institutional Review Board Statement: Not applicable.

Informed Consent Statement: Not applicable.

Data Availability Statement: Not applicable.

Conflicts of Interest: The authors declare no conflict of interest.

Sample Availability: Samples of the compounds are not available from the authors.

References

1. Alvarado-Cárdenas, L.O.; Lozada-Pérez, L. A New Species of *Mandevilla* (Apocynaceae; Apocynoideae) from Mexico. *Phytotaxa* **2017**, *319*, 93. [[CrossRef](#)]
2. Endress, M.E.; Meve, U.; Middleton, D.J.; Liede-Schumann, S. Apocynaceae. In *Flowering Plants. Eudicots*; Springer International Publishing: Cham, Switzerland, 2018; pp. 207–411.
3. Morales, J.F.; de Morais, I.L. Studies in the Neotropical Apocynaceae LV: A New *Mandevilla* from Bahia, Brazil, with Notes on the Diversity of the Genus. *Syst. Bot.* **2020**, *45*, 183–189. [[CrossRef](#)]
4. da Silva-Monteiro, F.K.; de Morais-Rodrigues, E.; Manguiera-do Nascimento, Y.; Miranda-de Melo, J.I. Primer Registro de *Mandevilla dardanoi* (Apocynaceae) Para El Estado de Paraíba, Brasil. *Rev. Mex Biodivers.* **2017**, *88*, 755–758. [[CrossRef](#)]
5. Cordeiro, S.Z.; Sato, A.; Arruda, R.; de Oliveira Arruda, R.D.C.; Simas, N.K. Volatile Compounds of *Mandevilla guanabarica* (Apocynoideae, Apocynaceae) from Three Restingas in Rio de Janeiro, Brazil. *Biochem. Syst. Ecol.* **2012**, *45*, 102–107. [[CrossRef](#)]
6. de Almeida, D.A.T.; Rosa, S.I.G.; da Cruz, T.C.D.; Pavan, E.; Sabino Damazo, A.; Soares, I.M.; Ascêncio, S.D.; Macho, A.; de Oliveira Martins, D.T. *Mandevilla longiflora* (Desf.) Pichon Improves Airway Inflammation in a Murine Model of Allergic Asthma. *J. Ethnopharmacol.* **2017**, *200*, 51–59. [[CrossRef](#)] [[PubMed](#)]
7. Ribeiro, R.V.; Mariano, D.B.; Arunachalam, K.; Soares, I.M.; de Aguiar, R.W.S.; Ascêncio, S.D.; Marlon, R.; Colodel, E.M.; de Oliveira Martins, D.T. Chemical Characterization and Toxicological Assessment of Hydroethanolic Extract of *Mandevilla Velame Xylopodium*. *Rev. Bras. Farmacogn.* **2019**, *29*, 605–612. [[CrossRef](#)]
8. Tatsuzawa, F.; Yoshikoshi, A.; Takehara, A.; Suzuki, S. Flavonoids from the Flowers of *Adenium obesum* (Forssk.) Roem. & Schult., *Mandevilla sanderi* (Hemsl.) Woodson, and *Nerium oleander* L. (Apocynaceae). *Biochem. Syst. Ecol.* **2021**, *99*, 104347. [[CrossRef](#)]
9. Ferreira, L.L.D.M.; de Leão, V.F.; de Melo, C.M.; de Machado, T.B.; Amaral, A.C.F.; da Silva, L.L.; Simas, N.K.; Muzitano, M.F.; Leal, I.C.R.; Raimundo, J.M. Ethyl Acetate Fraction and Isolated Phenolics Derivatives from *Mandevilla moricandiana* Identified by UHPLC-DAD-ESI-MSn with Pharmacological Potential for the Improvement of Obesity-Induced Endothelial Dysfunction. *Pharmaceutics* **2021**, *13*, 1103. [[CrossRef](#)]
10. Konrath, E.L.; Strauch, I.; Boeff, D.D.; Arbo, M.D. The Potential of Brazilian Native Plant Species Used in the Therapy for Snakebites: A Literature Review. *Toxicon* **2022**, *217*, 17–40. [[CrossRef](#)]
11. Hammadi, R.; Kúsz, N.; Dávid, C.Z.; Mwangi, P.W.; Berkecz, R.; Szemerédi, N.; Spengler, G.; Hohmann, J.; Vasas, A. Polyoxypregnane Ester Derivatives and Lignans from *Euphorbia gossypina* var. *coccinea* Pax. *Plants* **2022**, *11*, 1299. [[CrossRef](#)]
12. Si, Y.; Sha, X.-S.; Shi, L.-L.; Wei, H.-Y.; Jin, Y.-X.; Ma, G.-X.; Zhang, J. Review on Pregnane Glycosides and Their Biological Activities. *Phytochem. Lett.* **2022**, *47*, 1–17. [[CrossRef](#)]
13. Abdel-Sattar, E.; Ali, D.E. Russelioside B: A Pregnane Glycoside with Pharmacological Potential. *Rev. Bras. Farmacogn.* **2022**, *32*, 188–200. [[CrossRef](#)]
14. Yan, Y.; Tang, P.; Zhang, X.; Wang, D.; Peng, M.; Yan, X.; Hu, Z.; Tang, L.; Hao, X. Anti-TMV Effects of Seco-Pregnane C₂₁ Steroidal Glycosides Isolated from the Roots of *Cynanchum paniculatum*. *Fitoterapia* **2022**, *161*, 105225. [[CrossRef](#)]
15. Wang, Y.-B.; Zhao, D.; Su, S.-S.; Chen, G.; Wang, H.-F.; Pei, Y.-H. Twelve New Seco-Pregnane Glycosides from *Cynanchum taihangense*. *Molecules* **2022**, *27*, 5500. [[CrossRef](#)]
16. El-Shiekh, R.A.; Hassan, M.; Hashem, R.A.; Abdel-Sattar, E. Bioguided Isolation of Antibiofilm and Antibacterial Pregnane Glycosides from *Caralluma quadrangula*: Disarming Multidrug-Resistant Pathogens. *Antibiotics* **2021**, *10*, 811. [[CrossRef](#)] [[PubMed](#)]
17. Yunes, R.A.; Brum, R.L.; Calixto, J.B.; Rimplert, H. Illustrol, a Seco-Norpregnane Derivative from *Mandevilla illustris*. *Phytochemistry* **1993**, *34*, 787–790. [[CrossRef](#)]
18. Liu, S.; Chen, Z.; Wu, J.; Wang, L.; Wang, H.; Zhao, W. Appetite Suppressing Pregnane Glycosides from the Roots of *Cynanchum auriculatum*. *Phytochemistry* **2013**, *93*, 144–153. [[CrossRef](#)]
19. Gan, H.; Xiang, W.-J.; Ma, L.; Hu, L.-H. Six New C₂₁ Steroidal Glycosides from *Cynanchum bungei* Decne. *Helv. Chim. Acta* **2008**, *91*, 2222–2234. [[CrossRef](#)]
20. Yunes, R.A.; Pizzolatti, M.G.; Sant'anab, A.E.G.; Hawkes, G.E.; Calixto, J.B. The Structure of Velutinol A, an Anti-Inflammatory Compound with a Novel Pregnane Skeleton. *Phytochem. Anal.* **1993**, *4*, 76–81. [[CrossRef](#)]
21. Watanabe, S.; Alexander, M.; Misharin, A.V.; Budinger, G.R.S. The Role of Macrophages in the Resolution of Inflammation. *J. Clin. Investig.* **2019**, *129*, 2619–2628. [[CrossRef](#)]
22. Fujiwara, N.; Kobayashi, K. Macrophages in Inflammation. *Curr. Drug Targets-Inflamm. Allergy* **2005**, *4*, 281–286. [[CrossRef](#)] [[PubMed](#)]
23. Cinelli, M.A.; Do, H.T.; Miley, G.P.; Silverman, R.B. Inducible Nitric Oxide Synthase: Regulation, Structure, and Inhibition. *Med. Res. Rev.* **2020**, *40*, 158–189. [[CrossRef](#)]

24. Holbrook, J.; Lara-Reyna, S.; Jarosz-Griffiths, H.; McDermott, M. Tumour Necrosis Factor Signalling in Health and Disease [Version 1; Referees: 2 Approved]. *F1000Res* **2019**, *8*, F1000 Faculty Rev-111. [[CrossRef](#)] [[PubMed](#)]
25. McInnes, I.B.; Gravalles, E.M. Immune-Mediated Inflammatory Disease Therapeutics: Past, Present and Future. *Nat. Rev. Immunol.* **2021**, *21*, 680–686. [[CrossRef](#)] [[PubMed](#)]
26. Dinarello, C.A. Overview of the IL-1 Family in Innate Inflammation and Acquired Immunity. *Immunol. Rev.* **2018**, *281*, 8–27. [[CrossRef](#)] [[PubMed](#)]
27. Kaneko, N.; Kurata, M.; Yamamoto, T.; Morikawa, S.; Masumoto, J. The Role of Interleukin-1 in General Pathology. *Inflamm. Regen.* **2019**, *39*, 12. [[CrossRef](#)]
28. Mattos, W.M.; Campos, M.M.; Fernandes, E.S.; Richetti, G.P.; Niero, R.; Yunes, R.A.; Calixto, J.B. Anti-Edematogenic Effects of Velutinol A Isolated from *Mandevilla velutina*: Evidence for a Selective Inhibition of Kinin B1 Receptor-Mediated Responses. *Regul. Pept.* **2006**, *136*, 98–104. [[CrossRef](#)]
29. Tiffany, C.W.; Burch, R.M. Bradykinin Stimulates Tumor Necrosis Factor and Interleukin-1 Release from Macrophages. *FEBS Lett.* **1989**, *247*, 189–192. [[CrossRef](#)]
30. Cabral, B.; Gonçalves, T.A.F.; Abreu, L.S.; Andrade, A.W.L.; de Azevedo, F.D.L.A.A.; de Castro, F.D.; Tavares, J.F.; Guerra, G.C.B.; de Rezende, A.A.; de Medeiros, I.A.; et al. Cardiovascular Effects Induced by Fruit Peels from *Passiflora Edulis* in Hypertensive Rats and Fingerprint Analysis by HPLC-ESI-MSn Spectrometry. *Planta Med.* **2021**, *88*, 356–366. [[CrossRef](#)]
31. Espírito-Santo, R.F.; Meira, C.S.; dos Costa, R.S.; Souza Filho, O.P.; Evangelista, A.F.; Trossini, G.H.G.; Ferreira, G.M.; Velozo, E.d.S.; Villarreal, C.F.; Pereira Soares, M.B. The Anti-Inflammatory and Immunomodulatory Potential of Braylin: Pharmacological Properties and Mechanisms by in Silico, in Vitro and in Vivo Approaches. *PLoS ONE* **2017**, *12*, e0179174. [[CrossRef](#)]
32. Opretzka, L.C.F.; do Espírito-Santo, R.F.; Nascimento, O.A.; Abreu, L.S.; Alves, I.M.; Döring, E.; Soares, M.B.P.; Velozo, E.D.S.; Laufer, S.A.; Villarreal, C.F. Natural Chromones as Potential Anti-Inflammatory Agents: Pharmacological Properties and Related Mechanisms. *Int. Immunopharmacol.* **2019**, *72*, 31–39. [[CrossRef](#)] [[PubMed](#)]
33. Green, L.C.; Wagner, D.A.; Glogowski, J.; Skipper, P.L.; Wishnok, J.S.; Tannenbaum, S.R. Analysis of Nitrate, Nitrite, and [15N] Nitrate in Biological Fluids. *Anal. Biochem.* **1982**, *126*, 131–138. [[CrossRef](#)]